13
The Retinasensor: An In Vitro Tool to Study Drug Effects on Retinal Signaling

Elke Guenther, Thoralf Herrmann, and Alfred Stett

13.1 Introduction

Recent advances in growing electrically active cells on substrate-integrated microelectrode arrays (MEAs), either as cell cultures or in a tissue slice, have led to test systems in which cellular activity can be recorded acutely or up to several months. As the MEA technology can be applied to any electrogenic tissue (i.e., central and peripheral neurons, heart cells, and muscle cells), MEA biosensors are ideal in vitro systems to monitor both acute and chronic effects of drugs and toxins and to perform functional studies under physiological or induced pathophysiological conditions that mimic in vivo damages. By recording the electrical response at various locations on a tissue, a spatial map of drug effects at different sites may be generated, providing important clues about a drug's specificity.

In the following we describe a preparation of the vertebrate retina on microelectrode arrays to record local electroretinograms in vitro (microERG) under defined experimental conditions. We show that the so-called retinasensor is a suitable in vitro tool to easily and effectively assess effects of pharmacological compounds and putative therapeutics on retinal function. The major advantage of the preparation is that the retina together with the retinal pigment epithelium can be isolated as a whole by merely cutting the optic nerve without the necessity of slicing the tissue and thus damaging the cellular layers as in other in vitro preparations of the central nervous system.

13.2 The Retinasensor

13.2.1 The Electroretinogram

The retina is a peripheral, easily accessible part of the central nervous system that lines the back of the eye. All vertebrate retinas are composed of three layers of nerve cell bodies and two layers of synapses. The outer nuclear layer contains cell bodies of the photoreceptors, the rods and cones; the inner nuclear layer contains

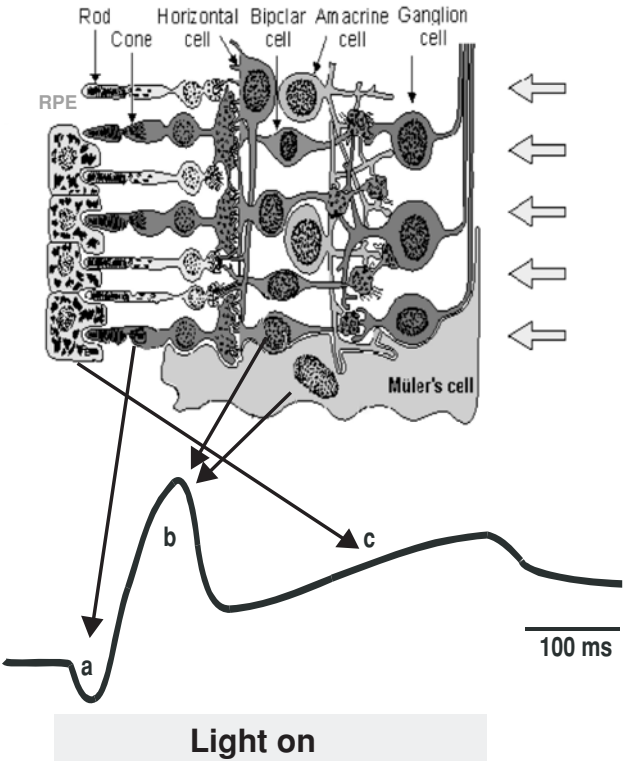

FIGURE 13.1. Top: Schematic representation of a retinal cross-section showing the assembly of all retinal neurons together with the retinal Müller glia cells and the retinal pigment epithelium. Bottom: Typical example of an electroretinogram (ERG) showing the characteristic waveform composed of the a-wave, the b-wave, and the c-wave induced by stimulating the retina with light. The different waves can be attributed to different retinal cell types or layers as indicated by the arrows.

cell bodies of the bipolar, horizontal, and amacrine cells; and the ganglion cell layer contains cell bodies of ganglion cells and displaced amacrine cells. Dividing these nerve cell layers are two neuropils where synaptic contacts occur (Polyak, 1941; Rodieck, 1973; Kolb, 1991; see Figure 13.1).

Incidence of light results in a complex signaling within these retinal neurones that is reflected in the electroretinogram (ERG). The ERG is a mass electrical response of the eye that is made up of several components. Since the early twentieth century, numerous studies have been performed on the origin and characteristics of the ERG. Einthoven and Jolly (1908) separated the light-induced ERG response into three waves, called the a-, b-, and c-waves. An additional wave recorded at the termination of the light stimulus was called the d-wave. Granit (1933) demonstrated that the a-, b-, and c-waves are the summed responses of three underlying basic components, named PI to PIII. The component analysis of Granit that won him the

Nobel Prize for Physiology or Medicine in 1954 has been modified slightly over the years but remains the basis for our understanding of the ERG.

ERGs have been recorded in different animal species (Steinberg et al., 1970; Kline et al., 1985; Newman, 1985; Hood and Birch, 1995; Lei and Perlman, 1999; Kapousta-Bruneau, 2000; Jamison et al. 2001) and clearly differ in amplitude and pattern. Some of this variability is due to species differences, particularly the relative densities of rods and cones, whereas technical factors such as duration and intensity of photostimulation and method of recording also affect the waveform. Nevertheless, ERG responses recorded from vertebrate species are characterized by the basic features of a negative a-wave followed by a positive b-wave and c-wave.

Retinal function can be affected by acute injuries, intoxication, or retinal diseases, resulting in visual impairment or blindness. Under these conditions, the shape and amplitude of an ERG is altered, making it of clinical value as a diagnostic tool. The ERG is a test used worldwide in ophthalmology to assess the status of the retina in human patients (Marmor and Zrenner, 1998) and in laboratory animals used as models of retinal disease (Kueng-Hitz, 2000; Bolz et al., 2001).

The clinical value of the ERG as a diagnostic tool comes from the fact that the different ERG waves can be attributed to distinct retinal layers or even cell types (see Figure 13.1). It is known that the a-wave is generated by the photoreceptors (Tomita, 1950; Brown and Wiesel, 1961; Sillman et al., 1969) and the c-wave originates in the retinal pigment epithelium (Noell, 1954; Steinberg et al., 1970; Marmor and Hock, 1982). The b-wave is formed in retinal cells that are postsynaptic to the photoreceptors but its exact source is still under dispute. However, it is agreed that large parts are generated by ON-bipolar cells (Gurevich and Slaughter, 1993; Sieving et al., 1994), and there is also a participation of Mueller glia cells (Miller and Dowling, 1970). With a proper analysis of the ERG waves under physiological and pathophysiological conditions it is thus possible to dissect out the functional integrity of different retinal structures and to understand information-processing mechanisms and/or the sites of retinal disorders and dysfunction. In the following, a new experimental system is described that for the first time allows multi-site recording of ERGs in vitro.

13.2.2 Practical Approach

13.2.2.1 Tissue Preparation

One- to three-day-old chickens were light-adapted and killed by decapitation. Light adaptation ensures that the pigment epithelium (RPE) is tightly attached to the retina due to the protrusion of the photoreceptor outer segments into the RPE. The eyes were dissected immediately after enucleation by hemisection of the upper third of the eye-cup with a sharp razor blade. The lens and vitreous were carefully removed. Square segments of 4 mm^2 were cut out from the eye-cup and the neural retina and the pigment epithelium was gently removed from the underlying tissue. One sample was placed ganglion cell side down (Figure 13.2) onto a MEA chip

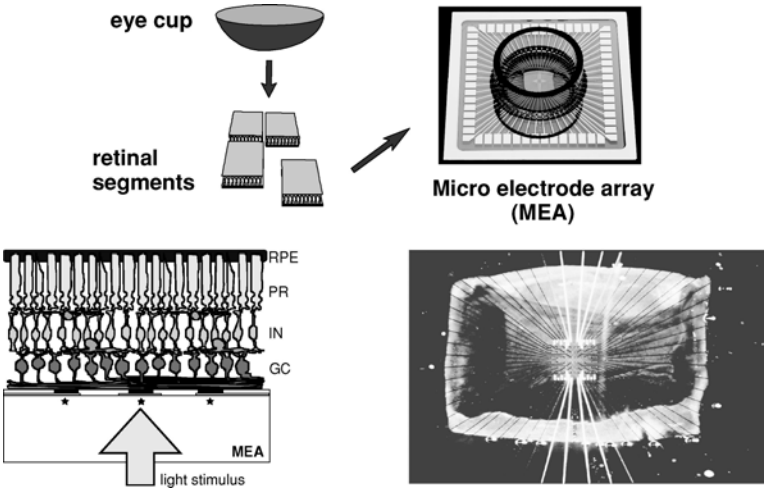

FIGURE 13.2. Preparation of samples of the chicken retina on a microelectrode array. The retina is placed ganglion cells down onto the MEA chip (lower left). The retina together with the retinal pigment epithelium (RPE) seen through the translucent MEA chip. The brownish color comes from the pigmentation of the RPE (lower right).

consisting of 60 surface-integrated planar electrodes (TiN, diameter 30 μm, rectangular arrangement, interelectrode spacing 200 μm). A recording chamber was glued onto the glass chip to allow superfusion of the tissue. The sample was superfused at a rate of 1 ml/min (syringe pump, flow 400 μl/m, TSE, Bad Homburg, Germany) with bubbled (95% O_2, 5% CO_2) standard Ringer solution (in mM: 120 NaCl, 5 KCl, 3 $CaCl_2$, 1 $MgSO_4$, 25 $NaHCO_3$, 25 glucose, 1 NaH_2PO_4; osmolarity 340 mOsm, pH 7.5). The MEA chip was mounted to a MEA stage with integrated heating (MCS, Reutlingen, Germany) and placed onto the table of an inverted microscope (Zeiss Axiovert 10, Zeiss AG, Oberkochen, Germany). Experiments were performed at a temperature of 35°C. The remaining samples were stored in bubbled ringer solution on a heating plate and kept in darkness for further use.

13.2.2.2 Setup

After at least 30 min of dark adaptation, an experiment was started. Full-field stimulation with light impulses of defined length and frequency was performed with the halogen lamp of the microscope (100 W) and an electromagnetic shutter. The light was projected through the objectives of the inverted microscope homogeneously onto the retinal sample. Light intensity and wavelength were controlled by neutral density and color filters (optical filters, Schott AG, Mainz, Germany) manually inserted into the optical pathway. Full-field light intensity on the retina level without a filter was 100 mW/cm^2 for white light, 20 mW/cm^2 for blue light, and 40 mW/cm^2 for red light. A schematic of the optical path and the recording setup is shown in Figure 13.3.

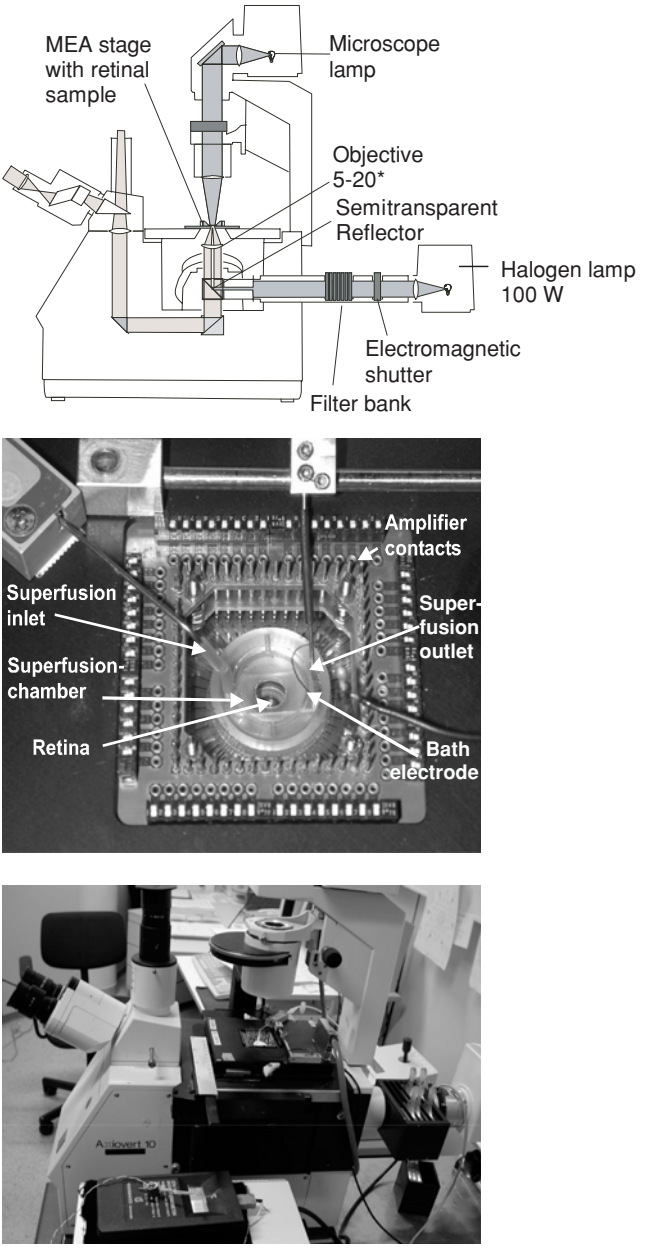

FIGURE 13.3. Schematic representation of the optical path through an inverted microscope (top). The MEA chip with the perfusion chamber containing the retina is placed on the microscope stage (middle). View on the recording setup (bottom).

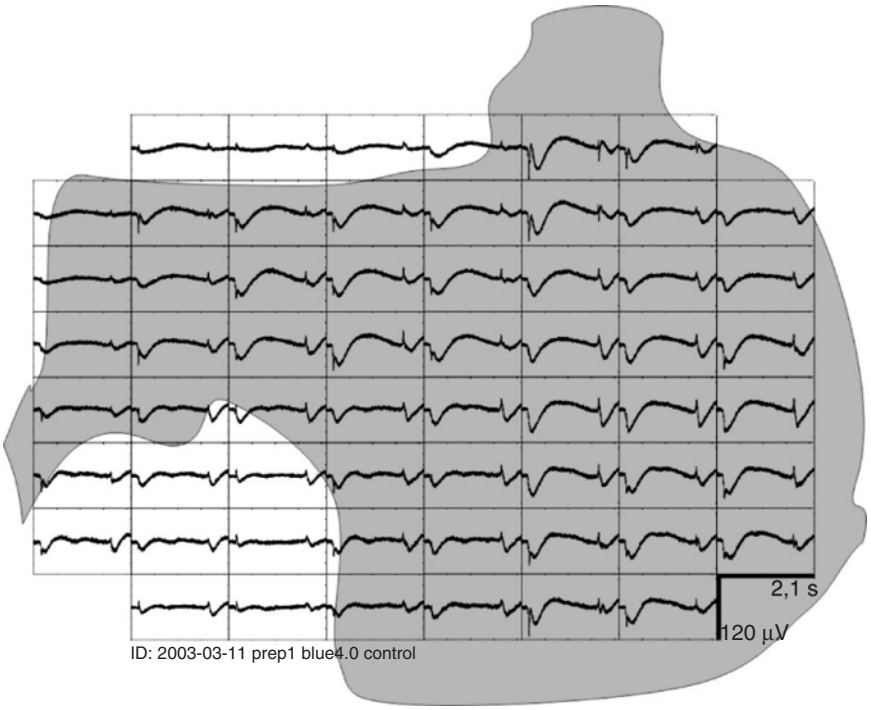

FIGURE 13.4. Micro-ERGs induced by light stimulation and recorded on 60 electrode sites in parallel. Shading outlines the retina/RPE complex whereas, in the white area, both tissues fell apart and only the retina was present. Typical micro-ERGs with good signal-to-noise ratios were only recorded in the central part within the retina/RPE complex.

13.2.2.3 Micro-ERG Recording

Micro-electrode recordings of retinal activity were obtained from up to 60 retinal sites with a MEA60 system (Multi Channel Systems MCS GmbH, Reutlingen, Germany) with a bandwidth of 0.5 to 2.8 kHz and a gain of 2300. For analysis, the responses to five consecutive stimuli were averaged at each site. Figure 13.4 shows a typical recording of local micro-ERGs at 60 electrode sites in parallel as displayed on the computer screen with the McRack software (MCS, Reutlingen, Germany). The whole electrode field (1.4×1.4 mm^2) was covered by the retinal sample, but only in the grey shaded area was the retinal pigment epithelium closely attached to the retina. The micro-ERGs are most pronounced in the central part of the retina/RPE preparation whereas the signals deteriorate at its marginal zones or in the area with retina only (white electrode area in Figure 13.4).

In Figure 13.5, light-induced signals on a single electrode are displayed. With adequate filter setting, either micro-ERGs (0.5 to 100 Hz) or ganglion cell spikes (200 Hz to 2.8 kHz) can be recorded. The micro-ERG in vitro clearly shows a light-on and light-off response and the light-on response is composed of the three main

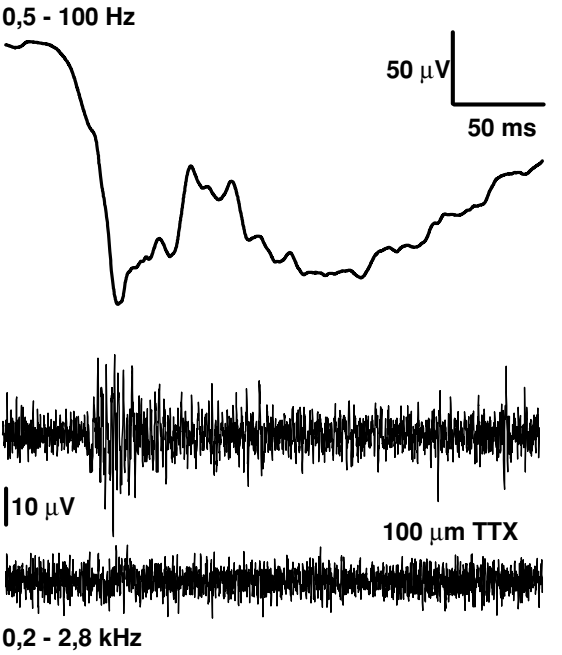

FIGURE 13.5. ON responses of the chicken micro-ERG recorded at one electrode. Top: slow wave component (average of five sweeps); bottom: spike recording of ganglion cell activity, filter settings as indicated. The transient ON-response of ganglion cells was blocked by the sodium channel antagonist TTX.

components, the a-, b-, and c-waves (Figure 13.5 top) as in a typical ERG recording in vivo. Compared to ERG studies on the chicken performed in vivo, the amplitude of the b-wave is smaller in our in vitro preparation (Wioland et al., 1990; Schwahn et al., 2000). This may be attributed to differences in the light stimulation and the method of recording (Perlman, 2003). However, we have observed the relation of Mg^{2+} and Ca^{2+} in the bath solution to be a most crucial factor for the size of the b-wave. Largest b-waves in vitro were obtained with 3 mM Ca^{2+} and 1 mM Mg^{2+}. Light-induced micro-ERG recordings were performed up to two hours with one retinal sample.

In contrast with ERG recordings in vivo, the retinasensor preparation additionally allows the recording of retinal ganglion cell (RGC) activity (Figure 13.5, bottom). Because the retina is placed with the ganglion cell site down onto a MEA, the electrodes are in direct contact with either the RGC bodies or axons, and ON- and OFF-RGC spikes were recorded using a highpass filter. As in patch-clamp recordings of RGCs in a retinal slice, RGC spike activity was blocked with the sodium channel blocker TTX applied to the superfusion solution (Schmid and Guenther, 1998), additionally demonstrating the vitality of the preparation.

A clear dependence on the intensity of the light stimulus was observed for the micro-ERGs. Amplitudes of the micro-ERG components increased and kinetics

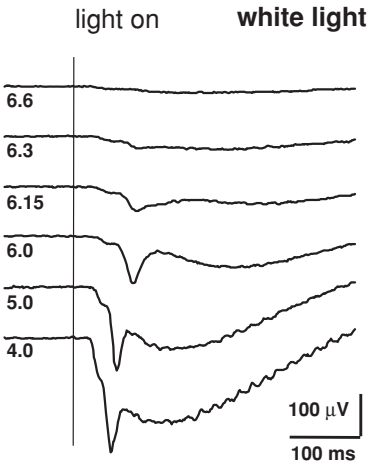

FIGURE 13.6. Light-dependence of micro-ERGs. Numbers on the right indicate the attenuation of light by neutral density filters in log units.

became faster with increasing intensity of a white light projected onto the retina (Figure 13.6). These light-dependent alterations are comparable to what has been reported for human and animal ERG recordings in vivo. However, overall light sensitivity depends on the species, the way the light is projected onto the retina, and, in vivo, how much of the light reaches the retina through the optic apparatus of the eye. Because light intensity in vivo is measured at the level of the cornea and not of the retina as in vitro, in vivo and in vitro data cannot directly be compared in terms of absolute sensitivities.

Lowering the temperature of the retina preparation from 35°C to 26°C had profound effects on the a-wave and b-wave amplitude whereas the c-wave amplitude was almost not affected (Figure 13.7). Again, this is in accordance with observations made in vivo in both chicken and mammals (Ookawa, 1970; Mizota and Adachi-Usami, 2002).

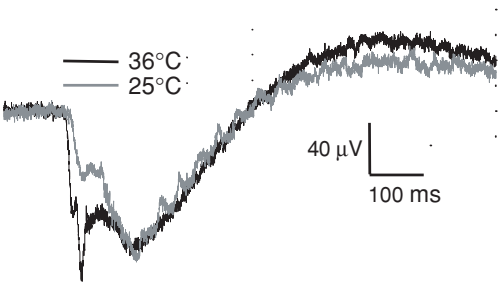

FIGURE 13.7. Temperature sensitivity of micro-ERG components.

13.2.3 *Pharmacological Characterization of Micro-ERGs*

In order to evaluate if drug-induced alterations of the ERG waveform can be detected with the retinasensor, 2-Amino-4-phosphonobutanoic acid (AP-4) was applied to the bath medium. AP-4 is a selective agonist at metabotrobic glutamate receptors of type 6 (mGluR6). In the retina, mGluR6 receptors are exclusively expressed on ON-bipolar cells. In darkness, when photoreceptors release glutamate, activation of mGluR6 produces a hyperpolarization of the postsynaptic ON-bipolar cells by closing a cation channel in the cell membrane. In contrast, with light exposure, when glutamate is no longer released, mGluR6 receptors are inactive, the cation channels open, and ON-bipolar cells are depolarized (Slaughter and Miller, 1981; Nawy and Jahr, 1990). If mGluR6 is activated with AP-4, ON-bipolar cells are hyperpolarized even in the presence of light. Thus, after a light stimulus, ON-bipolar cells should no longer contribute to the b-wave of the micro-ERG, and b-wave amplitude should be smaller with AP-4 than without. This is exactly what we observed when applying AP-4 to our in vitro preparation (Figure 13.8), indicating that the retinasensor is a suitable tool to analyze drug effects on retinal function. As in other retinal in vitro recordings, the AP-4 effect on the micro-ERG was reversible after washing the retina with normal ringer solution.

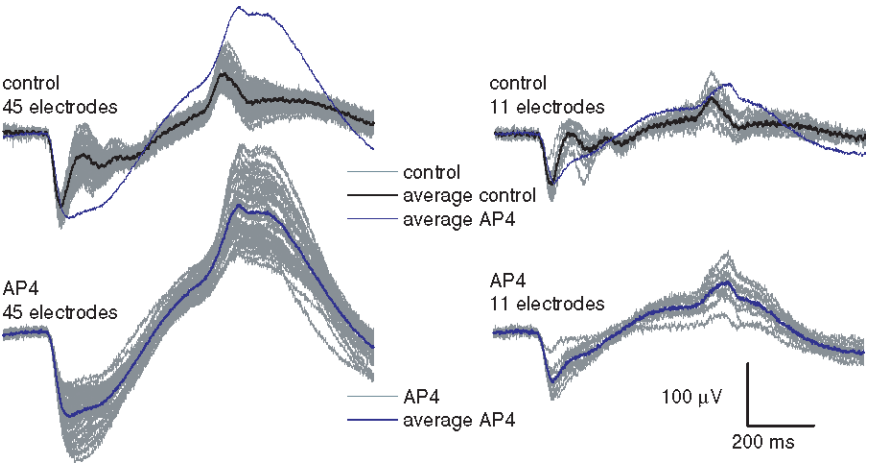

FIGURE 13.8. Effect of the mGluR6 agonist AP-4 on micro-ERG. Top row: control recordings obtained before application of 100 µM AP4; bottom row: recordings under exposure of the sample to AP4. In the given example, two principle waveforms of the recorded micro-ERG could be separated (left, right). The grey traces are individual recordings from a number of electrodes; each trace is the average of 30 recordings. The bold lines mark the average of the recordings from the given number of electrodes (black: average control, blue: average AP4). Stimulated with white light, 100 mW/cm^2. For comparison reasons, the averaged AP4 response is overlaid on the control recordings. The effect is reversible after washing (data not shown).

13.3 Summary and Conclusion

An in vitro preparation of the chicken retina was established on multi-electrode arrays. The so-called retinasensor allows the multi-site recording of micro-ERGs for hours and has been shown to be sensitive enough to assess drug effects on retinal function. The advantage of the system is that the retina can be isolated together with the retinal pigment epithelium as a whole by merely cutting the optic nerve. In contrast with other brain preparations, slicing of the tissue can be avoided and thus no damaged cells are present at the electrode–tissue interface that would interfere with the stimulation of healthy cell layers. A further advantage of the retinasensor is the recording of both micro-ERGs and ganglion cell activity. Because retinal ganglion cells do not contribute much to the ERG, additional information on the status of ganglion cells can be provided with the retinasensor as compared to ERG recordings in vivo. Taken together, the retinasensor offers a new assay system to reliably assess retinal function and dysfunction in vitro.

References

Bolz, H., von Brederlow, B., Ramirez, A., Bryda, E.C., Kutsche, K., Nothwang, H.G., Seeliger, M., C.-Salcedó Cabrera, M., Caballeró Vila, M., Pelaez Molina, O., Gal, A., and Kubisch, C. (2001). Mutations in cadherin-23 (otocadherin), a novel member of the cadherin gene family, cause Usher syn-drome type 1D. *Nat. Gene.* 27: 108–112.

Brown, K.T., and Wiesel, T.N. (1961a). Analysis of the intraretinal electroretinogram in the intact cat eye. *J. Physiol. (London)* 158: 229–256.

Brown, K.T., and Wiesel, T.N. (1961b). Localization of origins of electroretinogram components by intraretinal recording in the intact cat eye. *J. Physiol. (London)* 158: 257–280.

Einthoven, W., and Jolly, W.A. (1908). The form and magnitude of the electrical response of the eye to stimulation by light at various intensities. *Quaterly J. Exp. Physiol.* 1: 373–416.

Granit, R. (1933). The components of the retinal action potential in mammals and their relation to the discharge in the optic nerve. *J. Physiol. (London)* 77: 207–239.

Gurevich, L., Slaughter, M. M. (1993). Comparison of the waveforms of the ON bipolar neuron and the b-wave of the electroretinogram. *Vis. Res.* 33: 2431–2435.

Hood, D.C. and Birch, D.G. (1995). Phototransduction in human cones measured using the a-wave of the ERG. *Vis. Res*. 35: 2801–2810.

Jamison, J.A., Bush, R.A., Lei, B., and Sieving, P. (2001). Characterization of the rod photoresponse isolated from the dark-adapted primate ERG. *Vis. Neurosci*. 18: 445–455.

Kapousta-Bruneau, N.V. (2000). Opposite effects of $GABA_A$ and $GABA_C$ receptor antagonists on the b-wave of ERG recorded from the isolated rat retina. *Vis. Res*. 40: 1653–1665.

Kline, R.P., Ripps, H., and Dowling, J.E. (1985). Light-induced potassium fluxes in the skate retina. *Neuroscience* 14: 225–235.

Kolb, H. (1991). The neural organization of the human retina. In: Heckenlively, J.R. and Arden, G.B., eds., *Principles and Practices of Clinical Electrophysiology of Vision.* Mosby Year Book, St. Louis, pp. 25–52.

Kueng-Hitz, N., Grimm, C., Lansel, N., Hafezi, F., He, L., Fox, D.A., Reme, C.E., Niemeyer, G., and Wenzel, A. (2001). The retina of c-fos-/-mice: electrophysiologic, morphologic and biochemical aspects. *Invest. Ophthalmol. Vis. Sci*. 41(3): 909–916.

Lei, B. and Perlman, I. (1999). The contribution of voltage- and time-dependent poassium conductances to the electroretinogram in rabbits. *Vis. Neurosci*. 16: 743–754.

Marmor, M.F. and Zrenner, E. (1998). Standard for clinical electroretinography. *Doc. Ophthalmol.* 97: 143–156.

Miller, R.F., and Dowling, J.E. (1970). Intracellular responses of the Müller (glial) cells of the mudpuppy retina: their relation to the b-wave of the electroretinogram. *J. Neurophysiol.* 33: 323–341.

Mizota, A. and Adachi-Usami, E. (2002). Effect of body temperature on electroretinogram of mice. *Invest. Ophthalmol. Vis. Sci*. 43(12): 3754–3757.

Nawy, S. and Jahr, C.E. (1990). Suppression by glutamate of cGMP-activated conductance in retinal bipolar cells. *Nature* 346: 269–271.

Newman, E.A. (1985). Current source-density analysis of the b-wave of frog retina. *J. Neurophysiol*. 43: 1355–1366.

Noell, W.K. (1954). The origin of the electroretinogram. *Am. J. Ophthalmol.* 30: 78–90.

Ookawa, T. (1971). Effects of acute hypothermia on the chick ERG. *Experientia* 27(4): 405–407.

Perlman, I. (2003). The electroretinogram. http://webvision.med.utah.edu, Part XI.

Polyak, S.L. (1941). *The Retina*. University of Chicago Press, Chicago.

Rodieck, R.W. (1973). *The Vertebrate Retina: Principles of Structure and Function*. W.H. Freeman, San Francisco.

Schmid, S., and Guenther, E. (1998). Alterations in channel density and kinetic properties of the sodium current in retinal ganglion cells of the rat during in vivo differentiation. *Neuroscience* 85(1):249–258.

Schwahn, H.N., Kaymak, H., and Schaeffel, F. (2000). Effects of atropine on refractive development, dopamine release, and slow retinal potentials in the chick. *Vis. Neurosci*. 17(2): 165–176.

Sieving, P.A., Murayama, K., and Naarendorp, F. (1994). Push-pull model of the primate photopic electroretinogram: A role for hyperpolarizing neurons in shaping the b-wave. *Vis. Neurosci.* 11: 519–532.

Sillman, A.J., Ito, H., and Tomita, T. (1969a). Studies on the mass receptor potential of the isolated frog retina. I. General properties of the response. *Vis. Res.* 9: 1435–1442.

Sillman, A.J., Ito, H., and Tomita, T. (1969b). Studies on the mass receptor potential of the isolated frog retina. II. On the basis of the ionic mechanism. *Vis. Res.* 9: 1443–1451.

Slaughter, M.M. and Miller, R.F. (1981). 2-amino-4-phosphobutyric acid: A new pharmacological tool for retina research. *Science* 211: 182–184.

Steinberg, R.H., Schmidt, R., and Brown, K.T. (1970). Intracellular responses to light from cat pigment epithelium: Origin of the electroretinogram c-wave. *Nature* 227: 728–730.

Tomita, T. (1950). Studies on the intraretinal action potential. I. Relation between the localization of micropipette in the retina and the shape of the intraretinal action potential. *Jap. J. Physiol.* 1: 110–117.

Wioland, N. and Rudolf, G. (1991). Light and dark induced variations of the c-wave voltage of the chicken eye after treatment with sodium aspartate. *Vis. Res*. 31(4): 643–648.